# Journal Pre-proof


Characterization and analysis of filled knitted fabric formworks for advanced manufacturing of composite structures

Diddyer Barajas, Eduardo Pereira, Vítor Cunha, Filipa Monteiro, Luclécia Silva, Andrea Zille

PII: S2666-1659(23)00097-2

DOI: https://doi.org/10.1016/j.dibe.2023.100215

Reference: DIBE 100215

To appear in: *Developments in the Built Environment*

Received Date: 14 February 2023

Revised Date: 28 July 2023

Accepted Date: 17 August 2023

Please cite this article as: Barajas, D., Pereira, E., Cunha, Ví., Monteiro, F., Silva, Luclé., Zille, A., Characterization and analysis of filled knitted fabric formworks for advanced manufacturing of composite structures, *Developments in the Built Environment* (2023), doi: https://doi.org/10.1016/j.dibe.2023.100215.

# CHARACTERIZATION AND ANALYSIS OF FILLED KNITTED FABRIC FORMWORKS FOR ADVANCED MANUFACTURING OF COMPOSITE STRUCTURES

Diddyer Barajas[1], Eduardo Pereira[2], Vítor Cunha[3], Filipa Monteiro[4], Luclécia Silva[5], Andrea Zille[6]

**ABSTRACT**: An alternative construction methodology has been raising interest, consisting of employing fabrics as formworks. The implementation of flexible formworks allows the production of highly optimized organic structures, avoiding the use of unnecessary materials and consequently reducing construction loads, costs and waste. This study aims to integrate the experimental characterization of the mechanical behaviour of the knitted textiles used as formworks, the mechanical and deformational behaviour of the formworks while being filled with fresh mortar, and the numerical simulation of the multi-step process leading to the final structure. The integration of these different processes is essential for a sound design of this composite system as a construction strategy. To this end, this investigation identified several aspects, related to either experimental or computational mechanics

[1] PhD Student, ISISE, IB-S, University of Minho, School of Engineering, Campus de Azurém, 4800-058 Guimarães, Portugal. Email: id10429@alunos.uminho.pt

[2] Assistant Professor, ISISE, IB-S, University of Minho, School of Engineering, Campus de Azurém, 4800-058 Guimarães, Portugal. Email: eduardo.pereira@civil.uminho.pt

[3] Assistant Researcher, ISISE, IB-S, University of Minho, School of Engineering, Campus de Azurém, 4800-058 Guimarães, Portugal. Email: vcunha@civil.uminho.pt

[4] PhD Student, ISISE, IB-S, University of Minho, School of Engineering, Campus de Azurém, 4800-058 Guimarães, Portugal. Email: fmonteiro@civil.uminho.pt

[5] PhD Student, ISISE, IB-S, University of Minho, School of Engineering, Campus de Azurém, 4800-058 Guimarães, Portugal. Email: id10431@alunos.uminho.pt

[6] Associate Professor, Centre for Textile Science and Technology (2C2T), University of Minho, Department of Textile Engineering, Campus de Azurém, 4800-058 Guimarães, Portugal. Email: azille@det.uminho.pt

that are relevant to the topic and should be further investigated, with the aim of a future integrated material and structural design approach.

**KEYWORDS:** Digital image correlation (DIC); Finite element method (FEM); Knitted textiles; Membrane with large deformations; Textile formwork

## 1. INTRODUCTION

According to the Textile Institute, technical textiles are those used for their technical and performance properties rather than for their appearance or decorative features [1]. Depending on the material and manufacturing method, technical textiles can offer a wide range of physical, thermal and mechanical properties, e.g., lightness, high stiffness, corrosion resistance, fatigue resistance, insulation, conductivity and filtration [1–3]. For this reason, technical textiles are increasingly used for the manufacture of advanced structures in the automotive, aerospace, maritime, medical products and construction industries [2, 3].

The main methods of textile manufacturing are weaving, knitting, braiding and non-woven. Each of these methods has advantages that fit different fields of application [4, 5]. Woven fabrics are used in high-performance applications because the arrangement of the fibres gives them high strength and stiffness that prevents the growth of damage and deformation [1, 3, 6–8]. Braided fabrics are better adapted to the realization of large slender structures and intricate formworks, using mandrels in the manufacture, hence, this technique is optimal for the development of aerospace components [3, 5, 9–11]. Knitted fabrics allow the elaboration of elastic complex formworks in a single piece, minimizing the waste of material during production. In addition, they have a significant energy absorption capacity and can maintain a large portion of the initial resistance after damage [12–15]. Non-woven fabrics are made from the union of intermingled fibres, which makes their production fast and economical. This gives them enormous versatility, however, their mechanical properties are diminished compared to other types of textiles [1, 16].

In the construction industry, technical textiles have mainly been implemented to produce geotextiles with greater resistance to severe temperatures or climatic conditions, making them excellent for soil reinforcement [2, 17]. Likewise, some studies have focused on the use of technical textiles as reinforcement in concrete composite structures, where this type of light reinforcement can be manufactured to conveniently adapt to the direction of loads, while providing the structure with greater strength and stiffness [18–21]. Another application of technical textiles that is being studied consists of their implementation as flexible formworks, in which concrete is poured to create organic structures [17]. This construction method fetches a series of advantages at a structural, constructive, architectural, sustainability, and cost level that makes it very attractive. This encourages the study and development of tools to overcome the difficulties of its application in novel high-end industrial applications [22].

Some of the current main challenges for the commercial use of this construction method are : i) current numerical tools have not been sufficiently developed for the prediction of the behaviour of this type of structures;

ii) there is still no standardized methodology for the characterization of technical textiles in the construction industry; iii) the application of a form-finding procedure to predict the initial shape of the fabric formwork to reach the required shape when filled with cementitious mixture; iv) after obtaining the initial shape of the formwork, the patterns for cutting the fabric must be defined in order to reduce seams as much as possible. Consequently, there is the need for a comprehensive investigation to make fabric formwork a competitive construction technique with commercial applications based on robust experimental data [23].

This study recognizes the potential of knitted fabrics and represents a first contribution in a series of studies needed to support the development of a comprehensive methodology for implementing knitted textiles as formworks in the construction of structures with complex geometries. It addresses the challenges previously identified and contributes to the understanding of the behaviour of this type of structures, while identifying the topics that require further investigation. For this, the experimental development of mortar casting in a rectangular fabric formwork is proposed as a case study. This process was analysed and measured using non-contact approaches and later compared to the results obtained from numerical simulations using finite element method (FEM). The tools and techniques required for the development and analysis of such structures are investigated and discussed in this work, with a view on future optimization of the form-finding process and the required experimental characterization of the components.

The results of this study are significant for the integration of various processes involved in developing structures using knitted fabric formworks as a constructive methodology. Currently, the literature lacks studies that comprehensively address case studies involving: the mechanical characterization of the textile material of the formwork, ii) the implementation of computational strategies for predicting the behaviour of fabric formworks when they are precast with mortar, iii) the development of experimental tests to characterize the components of the system and iv) a methodology for comparing the experimental results and the predicted ones. This study fills that gap by providing a detailed investigation involving all these aspects necessary for the development of a standardized methodology. The results obtained provide insights into the shortcomings and areas for improvement in each of these processes.

## 2. EXPERIMENTAL STUDY OF A FABRIC FORMWORK

### 2.1. Casting of the fabric formwork

A rectangular fabric formwork 0.15 m wide and 1 m long was employed to investigate its behavior and free deformation process during mortar pouring. To fabricate this formwork, a weft-knitted fabric was first created with an electronic rectilinear loom using a textured polyester thread to form a locked mesh stitch with a density of

12 courses/cm by 9 wales/cm (see Figure 1a). This variation of the knitted manufacture technique was chosen in order to avoid excesive leakage of the mortar and also provide greater stiffness, due to its double bed stitch pattern.

Figure 1b depicts the knitting diagram, from bottom to top, the first row in red represents a plain knit structure created by the front needlebed of the knitting machine, advancing from left to right. During the return pass, the same type of structure is formed by the back needlebed, indicated by the green colour. These two structures, which were previously separated, are locked together through a double jersey loop, represented in yellow. Subsequently, this process is cyclically repeated according to the code illustrated in the Figure 1b. Then, the knitted fabric was sewn together along its bottom and lateral borders, in a running stitch using the same thread, forming the final formwork shape.

The experimental set-up involved suspending the fabric formwork by its upper edge, which was left open for mortar pouring, as depicted in Figure 2. Then, a self-compacting mortar mixture with an approximate density of 1940 kg/m3 was poured into the fabric formwork manually at an average rate of about 0.9 L/min, gradually and carefully, so that the load increased slowly and the formwork had time to adapt, without compromising the fresh state of the mortar. The entire process lasted 8 minutes, by which time the concrete had reached a height of 80 cm inside the fabric formwork.

To enhance the workability of the mortar, the superplasticizer Sika 3005 was incorporated as a chemical admixture. The specific proportions of the mixture are presented in Table 1. Additionally, a measuring tape was placed next to the fabric formwork to allow the visual assessment of the scale and the deformations during the experiment.

Progressive deformations were observed in the knitted fabric formwork as mortar was poured into it. These deformations arise mostly from the accommodation of fibres composing the internal structure of the material. Such mechanisms confer a high energy absorption capacity to this type of textile, without compromising the material's integrity [24]. Moreover, the incorporation of the locked mesh (double-bed) stitch technique in the fabric significantly enhanced its strength, as demonstrated by the experiment, in which no yielding or failure was observed at any point of the fabric formwork.

### 2.2. Analysis of surface deformations using particle tracking

The whole experiment was recorded with photographs taken at 5-second intervals by a high-resolution digital camera with a 36 Mpix full frame sized Complementary Metal-oxide-semiconductor sensor (CMOS 35.9 x 24 mm) and an objective lens with a focal length of 35 mm, to monitor the behaviour and deformations of the fabric formwork using digital image analysis (particle tracking). Compared to traditional measurement techniques,

this methodology has the possibility of capturing deformations in any direction on the surface of the fabric formwork. This is a great advantage, considering that the test is performed for the first time and its configuration allows the free deformation of the fabric formwork.

To start processing the results, the collected images were analysed and prepared using the open-source software for scientific image analysis called ImageJ [25]. The following steps were performed: i) changing the images to an 8-bit grayscale; ii) cropping images; iii) inverting the colours; iv) modifying the brightness and contrast. Thus, it was possible to reduce the size of the image sequence, focus attention on the fabric formwork and highlight points of interest in the experimental casting.

Then, the reference scale of the images was calibrated and set using the scale arranged next to the fabric formwork. The resulting image sequence was then processed using the TrackMate plugin in Fiji software [26]. Particle tracking analysis was performed on two regions of interest (RoI) of the formwork. RoI 1 is located closer to the support and RoI2 focused on the free end of the formwork. Both areas delimited by yellow rectangles are illustrated in Figure 3.

Limiting the area of analysis to specific regions rather than the entire image can be very beneficial in testing and determining the correct parameters to track the particles of interest. Afterwards, with each of the RoIs, the follow-up analysis was done separately: i) the simple Laplacian Gaussian filter was defined for both RoI 1 and RoI 2, ii) then, a segmentation process was performed, followed by a filtering of the unwanted points based on the quality threshold parameter. iii) finally, the simple Linear Assignment Problem (LAP) tracker was used to join points between subsequent images. In this way, the most representative tracks that describe the entire experimental test were obtained. The recognized trajectories were very few due to the variation of lighting and sudden movements, but they contain the necessary information to carry out comparative analysis with numerical models.

### 2.3. Surface deformations

A suitable examination on the selected tracks was performed to ensure that it always recognized the same point throughout all images, as during sudden movements of the formwork, the track was sometimes recognizing a closer point, instead of the original one. Figure 3b shows the tracks obtained for RoI 1, designated as R1a, and R1b and Figure 3c shows the tracks for RoI 2, called R2a and R2b. Also, some movement peaks in the transverse direction (perpendicular to gravity direction) of the formwork can be observed, which show the undesired effect of the movements occurring during the experiment caused by the mortar mass while filling in the formwork.

The tracks present a similar pattern in their behaviour, however the deformation in the longitudinal direction (along gravity direction) of the formwork is larger in the RoI 2 tracks compared to the RoI 1 tracks. This is because

the RoI 2 tracks are in the free end of the formwork, where there is the possibility of a greater freedom of deformation, while the tracks of RoI 1 are closer to the fixed end of the formwork at the top. On the other hand, the transverse deformation in the upper tracks (R1a and R1b) begins to increase as the height of the mortar approaches its location, which reflects a good correlation between the results obtained and the experimental test.

Relevant information regarding each track is summarized in Table 2, where the total number of points identified are presented, as well as the location of the starting point of each track with respect to the relative coordinate system (Figure 3a), and finally the total displacement in the longitudinal direction ($u_L$) and in the transverse direction ($u_T$).

## 3. KNITTED FABRIC – CONSTITUTIVE MODEL AND CHARACTERIZATION

### 3.1. Constitutive model

As mentioned in section 2.1, weft knitting technique was used to manufacture the fabric formwork with a textured polyester thread. This thread suits well the requirements of this research and the intention to conduct initial tests with readily available materials and study the behaviour of membrane-type elements of knitted textiles.

Based on the literature, knitted textiles are very heterogeneous structures and can be represented by means of a linear elastic orthotropic model with in-plane stresses, making following two assumptions: i) the way in which the textile is made results in a uniform structure in two orthogonal directions, where its mechanical properties retain the same symmetry of the geometry of the structure; ii) when out of the plane loads are applied, the textile material presents low deformations and the stresses along the thickness are negligible [27].

### 3.2. Experimental characterization

The elastic properties of the textile were characterized by performing tensile tests on specimens oriented in each of the main directions of the textile structure, according to the warp and weft directions (Figure 4). Five samples were taken from an excess portion of the fabric formwork, three in the transverse direction designated as A1, A2 and A3 and two in the longitudinal direction designated as B1 and B2.

The procedures for carrying out tensile tests on textiles are proposed by ASTM D2594M-21 [28] or ISO 13934-1:2013 [29]. Nonetheless, these standards are not developed for the particular characterization of knitted fabrics and are mainly focused on the characterization of fabrics in the field of the textile industry. Consequently, the test set-up and procedures were adapted, and the proposed dimensions for the specimens and some configurations for the test installation were taken as reference from [28, 29].

The test set-up, as shown in Figure 5, was composed of two steel grips, one fixed at the bottom and the other attached at the top to a hydraulic actuator, with a load capacity of 50 kN. As shown in Figure 4, rectangular

aluminium plates were glued at the edges of each side of the specimens using a cyanoacrylate adhesive, to guarantee a better fixation of the specimens inside the clamps used to grab the specimens at each edge, and thus avoid their slippage during the test.

The ISO 13934-1 standard specifies a procedure to characterize textile fabrics using a strip method, which includes the use of at least 5 test specimens in both transverse and longitudinal directions, with specific dimensions of 50 mm +/- 5 mm width and 200 mm gauge length. However, due to limited availability of materials, it was not possible to meet the recommended number of test specimens in this study. Nonetheless, to ensure compliance with the standard and maintain accurate reporting, the dimensions of each test specimen utilized have been documented in Table 3. On the other hand, due to the variability of the surface of knitted fabrics, the thickness was defined as the average of 12 measurements made with a pachymeter at different sections of the excess fabric. An average value of 1.83 mm was obtained, with a coefficient of variation of 4.13%.

Once the setting up of the specimen in the clamps was concluded, each specimen was subjected to a cyclic loading test. Three loading and unloading cycles were imposed to the specimen at a displacement rate of 2 mm/s. This test procedure was aimed at determining the variation of the axial deformability resulting from the rearrangement of the fibres in the textile structure.

3.2.1. *Tensile behaviour*

Figure 6 depicts the stress vs. strain responses ($\sigma$ - $\varepsilon$) obtained from the cyclical tests. The $\sigma$ - $\varepsilon$ curves corresponding to specimens A1, A2, A3 and B2 show a somewhat similar behaviour, where the completion of the cycles resulted in an increase of the specimens' axial stiffness, due to the readjustment of the fibres within the textile structure. Specimen B1 reached failure during the loading stage of the first cycle, since in this direction the textile shows greater stiffness, and the range of deformation was not duly reduced after executing the tests of specimens A1, A2 and A3. This procedural error was corrected for specimen B2, for which it was possible to obtain results for the characterization of the longitudinal direction of the textile

The tangent stiffness was calculated in order to describe the tensile behaviours as a representative measure of the axial deformability at each loading cycle of each specimen. For this estimation it was assumed that the stress level in the formwork lied between 50% to 75% of the maximum stress reached in each cyclic test, and because it effectively captures a significant part of the material's behaviour. The tangent stiffness obtained at the first loading cycle of each specimen will be subsequently adopted as the elasticity modulus in a linear elastic numerical simulation. This assumption is considered to approximate reasonably well the formwork filling test, since in this

case the fabric formwork was loaded for the first time. Consequently, the average tangent stiffnesses obtained in each direction, as presented in Table 4, were used for the following analyses.

Throughout the cyclic tests, careful observation of the jaws securing each sample revealed no signs of slippage. This finding was supported by a detailed analysis of stress vs. strain graphs, which exhibited no anomalies that would suggest slippage had occurred. Additionally, a thorough inspection of the aluminium plates placed at the ends of each specimen, following each cyclic test, revealed no evidence of slippage of any kind.

3.2.2. *Poisson's ratio*

Poisson's ratio is a property of great importance in the characterization of a material since it relates longitudinal with transverse deformations and describes the relation between other material elastic properties, such as the modulus of elasticity and the shear modulus. Different mathematical models and experimental procedures are established in the literature to determine the value of this parameter. However, the Poisson's ratio in this class of materials depends on different variables, such as the structure of the fabric, the properties of the fibre used, the magnitude of the applied load and the direction of application [30].

Due to the equipment available and the ease of execution, some specimens were monitored in order to better understand the multiaxial behaviour of the tested textiles. During the uniaxial tensile tests, a high-resolution camera with a 36 Mpix full frame sized CMOS sensor (35,9 x 24 mm) and an objective lens with a focal length of 70 mm, was used to capture images from the surface of the specimens at every 10 seconds. These images were subsequently used to produce the deformation fields at the surface of the specimens, by adopting the digital image correlation (DIC) technique. This methodology was implemented with specimens A2, A3 and B2, and with the results obtained it was possible to estimate the Poisson's ratio in both directions. Once the images were collected, these were processed using the GOM correlate software [31], which is widely used to analyse 2D and 3D deformations in materials.

The procedure executed in the software to analyse the strains of each specimen consisted in the creation of a surface in the centre of the sample, far from the region of influence of the grips and the curls on the textile edges (Figure 7). The surface component was created by implementing a facet size of 25 pixels with a point distance of 20 pixels. Regarding the calculation parameters, a bicubic subpixel interpolation was implemented to guarantee a more precise computation. Next, two orthogonal virtual clip gages were created for measuring the longitudinal and transverse elongations at the centre part of the specimen and throughout the first cycle of the uniaxial test, as illustrated in Figure 7. In addition to the strains, the surface component could also be used to observe the

longitudinal displacements field, identified by a colour scale on the right side, with the respective histogram of the number of points or facets identified in each displacement range.

Figure 8 shows the relationship between the strain in the transverse direction (Y strain) and the strain in the longitudinal direction (X strain) for each of the specimens analysed. The variable slope in this graph represents the Poisson's ratio, which tends to decrease as the specimens deform.

For the purpose of performing the numerical simulations of the formwork filling test conducted, the value of the Poisson's ratio implemented for the subsequent analysis was the one corresponding to the same range of stresses (between 50% to 75% of the maximum tensile stress) previously considered for the elasticity modulus. Therefore, for the transverse direction of the knitted textile, the test results of A2 and A3 were used and averaged, while for the longitudinal direction the test results of sample B2 were adopted. Table 4 summarizes the material properties obtained and used for the following analysis.

3.2.3. *Shear modulus*

Due to the behaviour of textile materials, special methodologies have been developed to determine the shear modulus [7, 32]. These procedures can require a significant amount of time and effort as well as the use of specialized laboratory equipment. Therefore, as a first approximation, it will be assumed that the shear modulus is negligible based on the a priori behaviour of the material and considering that a rigorous characterization of the material is outside the scope of this study. Finally, Table 4 presents the initial mechanical properties that will be adopted in the numerical models.

## 4. NUMERICAL SIMULATION OF THE FILLING PROCESS

### 4.1. Preliminary analysis of a flat membrane

The methodology followed in this study focused first on finding the most adequate process to establish the parameters, material properties, meshing method, definition of loads and finite element (FE) analysis procedures for simulating a flexible membrane. In order to simplify the problem in a first stage, before proceeding to the more complex geometry of the case study, a membrane with flat square geometry was considered. Therefore, a flat membrane with a regular simple geometry and the size of 1 m by 1 m was analysed under the framework of FEM using the software Abaqus [33]. Quadrilateral 4-node elements, designated in Abaqus as M3D4, with full integration scheme, were assigned to the mesh. A regular structured mesh with the size of 0.05 m was created, in order to have a moderately refined mesh. Regarding the boundary conditions, simple supports restraining the translational displacements along X, Y and Z axis were assigned along the four edges of the membrane (Figure 9). Additionally, a uniformly distributed load of 15.2 kPa perpendicular to the membrane surface was progressively

applied. This load is equivalent to the maximum hydrostatic pressure exerted by the mortar during casting in the experimental test, assuming that it has a specific density of 1940 kg/m3. The mechanical properties adopted for the membrane were those presented in Table 4.

As the phenomenon to be simulated shows a quasi-static behaviour, in which the inertial forces may be neglected, it can be both analysed using the "Dynamic Implicit" or "Dynamic Explicit" procedures of Abaqus. Consequently, a comparative analysis was carried out between these two procedures to determine which one achieved a better approximation of the behaviour with the lowest computational cost. From this preliminary study, convergence problems were found with both alternatives.

According to the literature, this issue could be associated with a lack of pre-tension in the membrane prior to the out-of-plane loading. It could also be associated to the absence of shear stiffness, since the shear modulus was prescribed as zero. The first hypothesis was tested by applying a small pre-tension to the membrane, by imposing an initial displacement at the supports of the membrane causing its pretension. However, the convergence problem still remained. In order to verify the second hypothesis, an approximation of the shear modulus was computed in a simplified way according to Eq. (1), by considering that the membrane is isotropic and using the elasticity moduli obtained experimentally. Although this calculation is not appropriate for an orthotropic material, it was adopted as an estimate to assess the influence of this parameter on the stability of the numerical modelling.

$$G = \frac{E_{ave}}{2(1 + \nu_{ave})} \quad (1)$$

The value of the shear modulus (G) was approximately 14 MPa, using for its calculation the average of the modulus of elasticity ($E_{ave}$) and Poisson's ratios ($\nu_{ave}$) presented in Table 4. When this parameter was modified, it was possible to obtain convergence without any type of warning, both in the implicit and the explicit procedure.

### 4.2. Numerical modelling of the fabric formwork

This model consists of a tubular fabric formwork with dimensions of 0.15 m wide by 1 m high, closely resembling the fabric formwork of the experimental case study. The formwork was suspended from the top with simple supports and the mortar cast process was simulated by a hydrostatic load that increased progressively until reaching a maximum height of 80 cm (Figure 10). This height was defined based upon experimental measurements.

#### 4.2.1. *Analysis using the dynamic implicit procedure*

Based on the implicit procedure, a model was created using a regular quadrilateral mesh of elements M3D4 with 0.02 m and with full integration. Simple supports were assigned to the fabric formwork on the upper edges and a hydrostatic pressure perpendicular to the inner face of the walls was imposed as a load. As the analysis should be quasi-static, the load was applied progressively with a small amplitude variation. However, when trying

to run the model a high computational cost has resulted, and a high number of warnings related to negative eigenvalues was found. This class of problem is common while using the standard solver and the implicit procedure when large deformations occur, this is well documented in the literature [34]. The solution typically proposed consists on using the explicit procedure to overcome these problems, since it presents a better computational performance when working with complex geometries and large deformations.

4.2.2. *Analysis using the dynamic explicit procedure*

The explicit procedure uses a time integration methodology that allows it to perform a large number of small time increments with reduced computational cost compared to the direct time integration method used by the Implicit procedure [34]. However, in the explicit solver there is no possibility to define a predefined hydrostatic pressure, unlike with the implicit solver. Therefore, in order to model a load of this type, it was necessary to program a routine that simulated the application of a variable hydrostatic pressure exerted by the rising level of the mortar on the fabric formwork during filling. The routine was implemented in Fortran language and was corroborated using a discrete model to compare both results.

Both the continuous FE model (CM) and the discrete FE model (DM) had the same geometry, mesh refinement and support conditions as the ones used in the Implicit procedure. For the CM model the Fortran routine was implemented according to a smooth function proposed in the Abaqus manual [35]. This function was designed to achieve a smooth transition between two successive values of the amplitude of a variable in a given time span. In this case, it was used to progressively increase the height of the fresh mortar, acting as the amplitude of the hydrostatic pressure exerted on the formwork over time. Therefore, the filling process of the fabric formwork was simulated with a controlled variation of the load, which is an explicit requirement for the quasi-static simulation. The smooth function given by Eqs. (2) y (3) may be represented as follows:

$$a_{(t)} = \begin{cases} A_i + (A_{i+1} - A_i)\xi^3(10 - 15\xi + 6\xi^2) & for\ t_i < t < t_{i+1} \\ A_{i+1} & for\ t \geq t_{i+1} \end{cases} \quad (2)$$

$$\xi = \frac{t - t_i}{t_{i+1} - t_i} \quad (3)$$

Where $a_{(t)}$ is the function that defines the variation of the amplitude and $t_i$ and $t_{i+1}$ are two consecutive values that define the time span in which the amplitude changes between the corresponding values $A_i$ and $A_{i+1}$.

On the other hand, in the DM model the formwork was subdivided into approximately thirty equal parts on which a uniform pressure was applied, with a magnitude equivalent to the average hydrostatic pressure corresponding to the average height of the subdivision. Finally, both models were observed to generate similar

results in terms of stresses and deformations, without any convergence problem, evidencing the correct functioning of the programming that simulates the load.

Subsequently, the results obtained from the CM numerical model were compared with the results obtained in the experimental mortar casting of the textile formwork. In general, it was observed that the longitudinal deformation of the numerical model was significantly lower than the one observed in the experiment. In order to verify the accuracy of simulating hydrostatic pressure and effectively represent the weight of the mortar, the authors calculated the reactions in the gravity direction at the support points of the fabric formwork. The sum of these reactions yielded a total of 139.6 N, corresponding to the weight equivalent of the fresh mortar. On the other hand, the weight of the fabric formwork after the mortar was poured during the experimental test, amounted to 134.3 N, resulting in a relative error of 4.0%. This discrepancy is likely attributed to minor differences between the actual formwork geometry and that employed in the simulation.

After verifying that the loads were being applied correctly to the formwork in the FE model, it was found that the stresses observed in the formwork were much lower than the ones assumed for estimating mechanical properties of the material (Table 4). This means that, in the numerical model, the stiffness adopted overestimated the real stiffness experienced in the experimental test, which is constant since the material was considered to be linear elastic. Consequently, the mechanical properties of the material were adjusted through an inverse analysis procedure, which iterated the estimation of the stiffness until the stress level for which the mechanical properties of the material were obtained coincided with the stress acting on the formwork in the numerical model. The mechanical properties obtained from this adjustment procedure are included in the Table 5. In this way, it was possible to obtain a better approximation of the longitudinal deformations in the numerical model.

## 5. COMPARISON OF EXPERIMENTAL AND NUMERICAL RESULTS

In a next step, a comparative analysis between the results obtained from the numerical model and the results of the experimental test was performed. In order to accomplish this comparison, four nodes were identified at the surface of the membrane in the numerical model. These nodes (Figure 11) are located approximately in the same positions as the points that were identified and tracked with the Image J software, using the sequence of images obtained during the experimental test (Figure 3b and Figure 3c).

From the numerical model, the displacements were obtained as a function of time, which can be related to the height of the filling mortar. In this way, the displacements in each direction obtained by analysing the experimental test results and the numerical ones are compared in Figure 12.

When comparing the longitudinal displacements, it can be observed that the numerical results approximate well both the magnitude of the displacements and the overall deformed shape obtained in the experimental test. The differences found may be attributed to the simplifications assumed when modelling the material behaviour and the parameters used for the constitutive model of the material, since a linear elastic orthotropic behaviour was assumed, while. As previously shown in Figure 6, the tensile tests showed that the deformability of the textile is not constant throughout the entire tensile response, and the behaviour of the material is non-linear, mainly for low stress levels, which was actually shown to be the case in the numerical model. The criterion for adjusting the modulus of elasticity was based on the maximum stress level present in the formwork. And in the case of the longitudinal modulus of elasticity, the formwork showed the greatest magnitude of stresses at the bottom, gradually reducing while approaching the top. For this reason, the estimated elasticity modulus generates a better approximation of the displacement of the traced points in the lower part of the formwork, while in the upper part the adopted elasticity modulus overestimates the actual deformability considering the acting stress level. Consequently, the numerically obtained displacements are smaller compared to the experimental results.

In contrast, when analysing the transverse displacements, significant differences were observed. In the numerical model out-of-plane deformations are generated as the load increases, causing transverse shrinkage displacements. These displacements are larger in the lateral zones, and therefore affect more the nodes tracked in the upper region since these were closer to the lateral zone. On the other hand, from the analysis carried out on the experimental results, transverse expansion displacements are observed, especially for the points of the lower region. These displacements were potentially caused by the seam in the lateral and lower regions of the formwork which, due to their higher stiffness, caused the formwork to twist and increase the transverse displacements, mainly in the lower region that is furthest from the support zone. In order to verify this hypothesis, the seam along the base and one of the sides of the formwork was simulated to replicate the manufacturing process of the physical fabric formwork. For this simulation, beam-type longitudinal elements with significantly higher stiffness than the formwork were utilized to represent the seams. These elements were assigned a mesh size identical to that of the membrane simulating the formwork and were attached together using a tie-type constraint, ensuring no relative movement between the formwork and the seams. The simulation results exhibited similar behaviour to that observed in the physical formwork, which experienced skewing during the pouring of the mortar. Although these results are not included in this study as the mechanical properties of the seams were not characterized, they do provide supporting evidence for the proposed hypothesis. Therefore, it is recommended that in future studies

involving the use of a seam, its mechanical properties should be adequately characterized in order to support the development of more precise numerical models.

The longitudinal displacements measured in the experimental test were less affected by conditions that notably hinder the measurement of transverse displacements. Therefore, for this case study, the vertical displacements turned out to be the parameters that best allowed the comparison and validation of the numerical model strategy. Furthermore, the simplification of the mechanical behaviour of the textile, assuming it is a linear elastic orthotropic material, leads to a good estimation of the displacements experienced by the formwork in the experimental test, with a computational cost of 5 minutes on a computer equipped with an Intel Core i7 processor and 12GB of RAM.

However, to improve the precision of numerical models, it is recommended to carry out an experimental campaign in line with the conditions experienced by the formworks in this construction methodology. Therefore, it is advisable to prepare and carry out biaxial tests, with an adequate number of specimens and the incorporation of the nonlinear behaviour of the material into the numerical models, especially for formworks subjected to significant stresses. Additionally, in the case of the adoption of seams for the preparation of the formwork, it is recommended to characterize its mechanical behaviour and incorporate it into the numerical models. This study shows the significant impact that seams can have on the behaviour of the formwork during the pouring of the mortar.

## 6. CONCLUSIONS

To summarize, the application of fabric formworks for the construction of geometrically complex structures is promising, and the numerical simulation of their behaviour during the casting stage seems feasible. This is very important since the correct geometrical definition and structural design are required. This research has shown that are several challenges that need to be dealt with, including the characterization of the textile material properties, the overcoming of the numerical problems deriving from the large deformations and loading typology, and the need to develop specific constitutive models that consider the nonlinear nature of the tensile behaviour of the knitted textiles. However, the results obtained are promising and show that it is possible to address these challenges even in a simplified way. All this is presented in detail below:

- As expected, due to the large deformations exhibited by the membrane and the nature of the applied load, it is appropriate to implement the explicit FEM analysis for the resolution of the quasi-static phenomenon in the numerical models. In contrast, it was confirmed that the implicit

procedure is not suitable for the resolution of this type of models under the conditions required in this construction methodology.

- The particle tracking technique has proven to be a suitable and practical tool for measuring deformations. However, its application requires better control of the conditions under which this type of experiment is performed. Therefore, future studies should consider the implementation of a high-resolution camera set with two or more cameras to accurately capture and measure 3D deformations while excluding unrelated movements.
- In this case study, approximating the behaviour of the fabric material to a linear elastic orthotropic model resulted in a good approximation since the stresses introduced into the fabric formwork were not very high. However, for cases where higher stresses are expected, it is important to simulate the non-linear behaviour of the material with a specifically developed constitutive model.
- It is important to emphasise that a comprehensive mechanical characterization of the knitted fabric is required to avoid convergence problems in the numerical models, i.e., biaxial tests. Therefore, the use of other methodologies for characterization is recommended, which guarantee more accurate and coherent mechanical properties.
- To mitigate excessive mortar leakage through the formwork pores, it is of great importance to explore alternative approaches, such as employing coating treatments on the knitted fabrics, especially when they exhibit significant mesh apertures. The use of double bed stitch patterns restricts the inherent advantages of the knitted fabrics, hindering its ability to create seamless geometries in a single piece.
- Finally, for future studies, it is recommended to extend, progressively, the scope of fabric formworks to more complex geometries or more demanding conditions in mortar casting, considering the integration of form- finding methodologies and the development of new numerical tools to analyse such structures. Once computational tools have reached sufficient development, they can be tested through larger-scale case studies, considering the following factors: (i) the use of stronger textile fibres to ensure better performance under higher loads, (ii) the planning of larger-scale structural components based on case studies previously reported in the literature that have utilized fabric formworks [36-38], and (iii) the scaling up of the mortar pouring mechanism to accommodate these new requirements.

**ACKNOWLEDGEMENTS**

This research was supported by the project ArchKnit, POCI-01-0247-FEDER-10227, co-funded by Fundo Europeu de Desenvolvimento Regional (FEDER), with Programa Operacional da Competitividade e Internacionalizacão do Portugal 2020 (COMPETE 2020).

**References**

[1] B. J. McCarthy, 'An overview of the technical textiles sector', in *Handbook of Technical Textiles*, Elsevier, 2016, pp. 1–20. doi: 10.1016/B978-1-78242-458-1.00001-7.

[2] J. HU, 'Introduction to three-dimensional fibrous assemblies', in *3-D Fibrous Assemblies*, Elsevier, 2008, pp. 1–32. doi: 10.1533/9781845694982.1.

[3] M. Bannister, 'Challenges for composites into the next millennium — a reinforcement perspective', *Compos Part A Appl Sci Manuf*, vol. 32, no. 7, pp. 901–910, Jul. 2001, doi: 10.1016/S1359-835X(01)00008-2.

[4] A. Dixit and H. S. Mali, 'Modeling techniques for predicting the mechanical properties of woven-fabric textile composites: a Review', *Mechanics of Composite Materials*, vol. 49, no. 1, pp. 1–20, Mar. 2013, doi: 10.1007/s11029-013-9316-8.

[5] M. Bannister and I. Herszberg, 'Advanced reinforcements', in *Resin Transfer Moulding for Aerospace Structures*, Dordrecht: Springer Netherlands, 1998, pp. 83–111. doi: 10.1007/978-94-011-4437-7_4.

[6] M. West, *The Fabric Formwork Book*. Routledge, 2016. doi: 10.4324/9781315675022.

[7] B. el Abed, S. Msahli, H. Bel Hadj Salah, and F. Sakli, 'Study of woven fabric shear behaviour', *Journal of the Textile Institute*, vol. 102, no. 4, pp. 322–331, Apr. 2011, doi: 10.1080/00405001003771226.

[8] J. Wang, P. Wang, N. Hamila, and P. Boisse, 'Mesoscopic analyses of the draping of 3D woven composite reinforcements based on macroscopic simulations', *Compos Struct*, vol. 250, Oct. 2020, doi: 10.1016/j.compstruct.2020.112602.

[9] L. Pei, Z. Xiao, L. Geng, J. Wu, F. Zhang, and Y. Sun, 'Surface parameters measurement for braided composite preform based on gray projection', *J Eng Fiber Fabr*, vol. 14, 2019, doi: 10.1177/1558925019887621.

[10] G. W. Melenka and J. P. Carey, 'Development of a generalized analytical model for tubular braided-architecture composites', *J Compos Mater*, vol. 51, no. 28, pp. 3861–3875, Dec. 2017, doi: 10.1177/0021998317695421.

[11] M. Frotscher, F. Schreiber, L. Neelakantan, T. Gries, and G. Eggeler, 'Processing and characterization of braided NiTi microstents for medical applications', *Materwiss Werksttech*, vol. 42, no. 11, pp. 1002–1012, Nov. 2011, doi: 10.1002/mawe.201100796.

[12] M. Duhovic and D. Bhattacharyya, 'Simulating the deformation mechanisms of knitted fabric composites', *Compos Part A Appl Sci Manuf*, vol. 37, no. 11, pp. 1897–1915, Nov. 2006, doi: 10.1016/j.compositesa.2005.12.029.

[13] S. Ramakrishna, 'CHARACTERIZATION AND MODELING OF THE TENSILE PROPERTIES OF PLAIN WEFT-KNIT FABRIC-REINFORCED COMPOSITES', 1997.

[14] T. D. Dinh, O. Weeger, S. Kaijima, and S. K. Yeung, 'Prediction of mechanical properties of knitted fabrics under tensile and shear loading: Mesoscale analysis using representative unit cells and its validation', *Compos B Eng*, vol. 148, pp. 81–92, Sep. 2018, doi: 10.1016/j.compositesb.2018.04.052.

[15] V. Schrank, M. Beer, M. Beckers, and T. Gries, 'Polymer-optical fibre (POF) integration into textile fabric structures', in *Polymer Optical Fibres: Fibre Types, Materials, Fabrication, Characterisation and Applications*, Elsevier Inc., 2017, pp. 337–348. doi: 10.1016/B978-0-08-100039-7.00010-5.

[16] D. J. Spencer, 'An introduction to textile technology', in *Knitting Technology*, Elsevier, 2001, pp. 1–6. doi: 10.1533/9781855737556.1.

[17] N. Ishmael, A. Fernando, S. Andrew, and L. Waterton Taylor, 'Textile technologies for the manufacture of three-dimensional textile preforms', *Research Journal of Textile and Apparel*, vol. 21, no. 4, pp. 342–362, Dec. 2017, doi: 10.1108/RJTA-06-2017-0034.

[18] H. Hasani, S. Hassanzadeh, M. J. Abghary, and E. Omrani, 'Biaxial weft-knitted fabrics as composite reinforcements: A review', *Journal of Industrial Textiles*, vol. 46, no. 7, pp. 1439–1473, 2017, doi: 10.1177/1528083715624256.

[19] T. Gries, M. Raina, T. Quadflieg, and O. Stolyarov, 'Manufacturing of Textiles for Civil Engineering Applications', in *Textile Fibre Composites in Civil Engineering*, Elsevier Inc., 2016, pp. 3–24. doi: 10.1016/B978-1-78242-446-8.00002-1.

[20] M. Mollaert, N. Cauberg, B. Parmentier, and D. Janssen, 'Fabric formwork for flexible, architectural concrete', in *Tailor Made Concrete Structures*, vol. 10, no. 2, CRC Press, 2008, pp. 168–168. doi: 10.1201/9781439828410.ch124.

[21] W. Hufenbach, R. Böhm, L. Kroll, and A. Langkamp, 'Theoretical and experimental investigation of anisotropic damage in textile-reinforced composite structures', *Mechanics of Composite Materials*, vol. 40, no. 6, pp. 519–532, Nov. 2004, doi: 10.1007/s11029-005-0022-z.

[22] J. J. Orr, A. P. Darby, T. Ibell, M. C. Evernden, and M. Otlet, 'Concrete structures using fabric formwork', *University of Cambridge*, vol. 89, no. 8, p. 26, 2017, doi: 10.17863/CAM.17019.

[23] F. Delijani, M. West, and D. Svecova, 'The evaluation of change in concrete strength due to fabric formwork', *Journal of Green Building*, vol. 10, no. 2, pp. 113–133, Jun. 2015, doi: 10.3992/jgb.10.2.113.

[24] P. Xue, T. X. Yu, and X. M. Tao, 'Tensile properties and meso-scale mechanism of weft knitted textile composites for energy absorption', *Compos Part A Appl Sci Manuf*, vol. 33, no. 1, pp. 113–123, 2002, doi: 10.1016/S1359-835X(01)00067-7.

[25] C. A. Schneider, W. S. Rasband, and K. W. Eliceiri, 'NIH Image to ImageJ: 25 years of image analysis', *Nat Methods*, vol. 9, no. 7, pp. 671–675, 2012, doi: 10.1038/nmeth.2089.

[26] J. Schindelin *et al.*, 'Fiji: an open-source platform for biological-image analysis', *Nat Methods*, vol. 9, no. 7, pp. 676–682, 2012, doi: 10.1038/nmeth.2019.

[27] Z. Jinyun, L. Yi, J. Lam, and C. Xuyong, 'The poisson ratio and modulus of elastic knitted fabrics', *Textile Research Journal*, vol. 80, no. 18, pp. 1965–1969, 2010, doi: 10.1177/0040517510371864.

[28] Standard Test Method for Stretch Properties of Knitted Fabrics Having Low Power, *ASTM D2594M*. 2021.

[29] Textiles-Tensile properties of fabrics-Part 1: Determination of maximum force and elongation at maximum force using the strip method, *ISO 13934-1*. 2013.

[30] N. Ezazshahabi, S. Mohammad, and H. Varkiyani, 'A Review on the Poisson's Ratio of Fabrics', 2020.

[31] 'GOM correlate'. GOM software, Braunschweig, Sep. 23, 2021.

[32] E. v. Morozov and V. v. Vasiliev, 'Determination of the shear modulus of orthotropic materials from off-axis tension tests', *Compos Struct*, vol. 62, no. 3–4, pp. 379–382, 2003, doi: 10.1016/j.compstruct.2003.09.008.

[33] 'Abaqus/CAE'. Dassault Systemes Simulia Corp., Johnston.

[34] Michael Smith, 'Choosing between implicit and explicit analysis', *Abaqus/CAE User's Manual*, 2017. https://abaqus-docs.mit.edu/2017/English/SIMACAEGSARefMap/simagsa-c-absadvexp.htm (accessed Dec. 02, 2022).

[35] Michael Smith, 'Amplitude Curves', *Abaqus/CAE User's Manual*, 2017. https://abaqus-docs.mit.edu/2017/English/SIMACAEPRCRefMap/simaprc-c-amplitude.htm (accessed Dec. 04, 2022).

[36] K. Kostova, T. Ibell, A. Darby, and M. Evernden, 'Form-Finding approach for flexibly formed concrete elements', *Proceedings of the Institution of Civil Engineers: Engineering and Computational Mechanics*, vol. 172, no. 3, pp. 96–105, 2019, doi: 10.1680/jencm.19.00005.

[37] J. J. Orr, T. J. Ibell, and A. P. Darby, 'Innovative concrete structures using fabric formwork', *Advances and Trends in Structural Engineering, Mechanics and Computation - Proceedings of the 4th International Conference on Structural Engineering, Mechanics and Computation, SEMC 2010*, no. April 2015, pp. 925–928, 2010.

[38] W. J. Hawkins *et al.*, 'Flexible formwork technologies – a state of the art review', *Structural Concrete*, vol. 17, no. 6, pp. 911–935, 2016, doi: 10.1002/suco.201600117.

525 **LIST OF TABLES**



531

532 Table 1. Mortar mixture proportions

| Cement (kg/m3) | Sand (kg/m3) | Fly ash (kg/m3) | Limestone filler (kg/m3) | Water (kg/ m3) | Chemical admixture (kg/m3) | w/c ratio |
|---|---|---|---|---|---|---|
| 484 | 726 | 169 | 169 | 312 | 27 | 0.65 |

533

534 Table 2. Data collected from the particle tracking analysis of the experimental test.

| Track | Number of spots | Location initial spot (mm) | | Final displacement (mm) | |
|---|---|---|---|---|---|
| | | $x_L$ | $x_T$ | $u_L$ | $u_T$ |
| R1a | 66 | 592.4 | 44.46 | 23.95 | 0.51 |
| R1b | 66 | 516.4 | 42.57 | 26.71 | 5.02 |
| R2a | 60 | 58.1 | 31.71 | 35.26 | 14.16 |
| R2b | 62 | 37.4 | 42.22 | 32.37 | 14.91 |

535
536

537 Table 3. Dimension of the specimens

| Specimen | A1 | A2 | A3 | B1 | B2 |
|---|---|---|---|---|---|
| **Length (mm)** | 151 | 165 | 158 | 193 | 193 |
| **Width (mm)** | 70 | 61 | 62 | 62 | 64 |

538

539 Table 4. Mechanical properties obtained from the characterization of the knitted fabric.

| **Direction** | **E (MPa)** | **ν** | **G (MPa)** |
|---|---|---|---|
| Transverse | 24.3 | 0.35 | - |
| Longitudinal | 53.8 | 0.45 | - |

540

541 Table 5. Mechanical properties obtained by inverse analysis.

| Direction | E (MPa) | ν | G (MPa) |
|---|---|---|---|
| Transverse | 3.63 | 0.74 | 1.90 |
| Longitudinal | 10.65 | 1.02 | |

542

**LIST OF FIGURES**

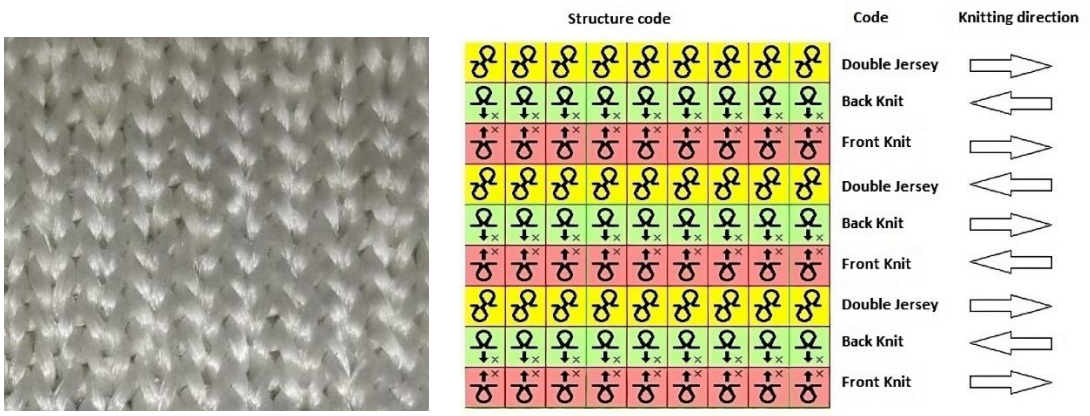


a) b)

Figure 1. a) Photograph of the implemented knitted fabric, b) Diagram in knitting notation, explaining the manufacture process of the fabric.

567

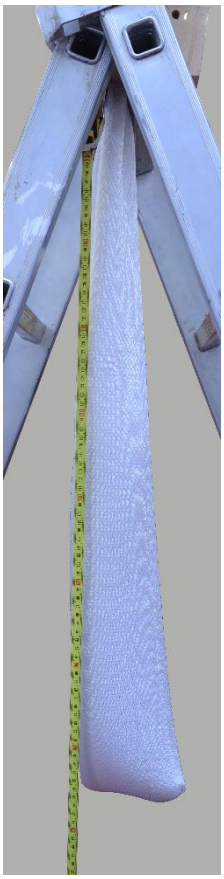

a)

b)

c)

Figure 2. a) Set-up of the fabric formwork casting, b) Detail of the casting process and c) Detail of the lower part of the formwork.

568

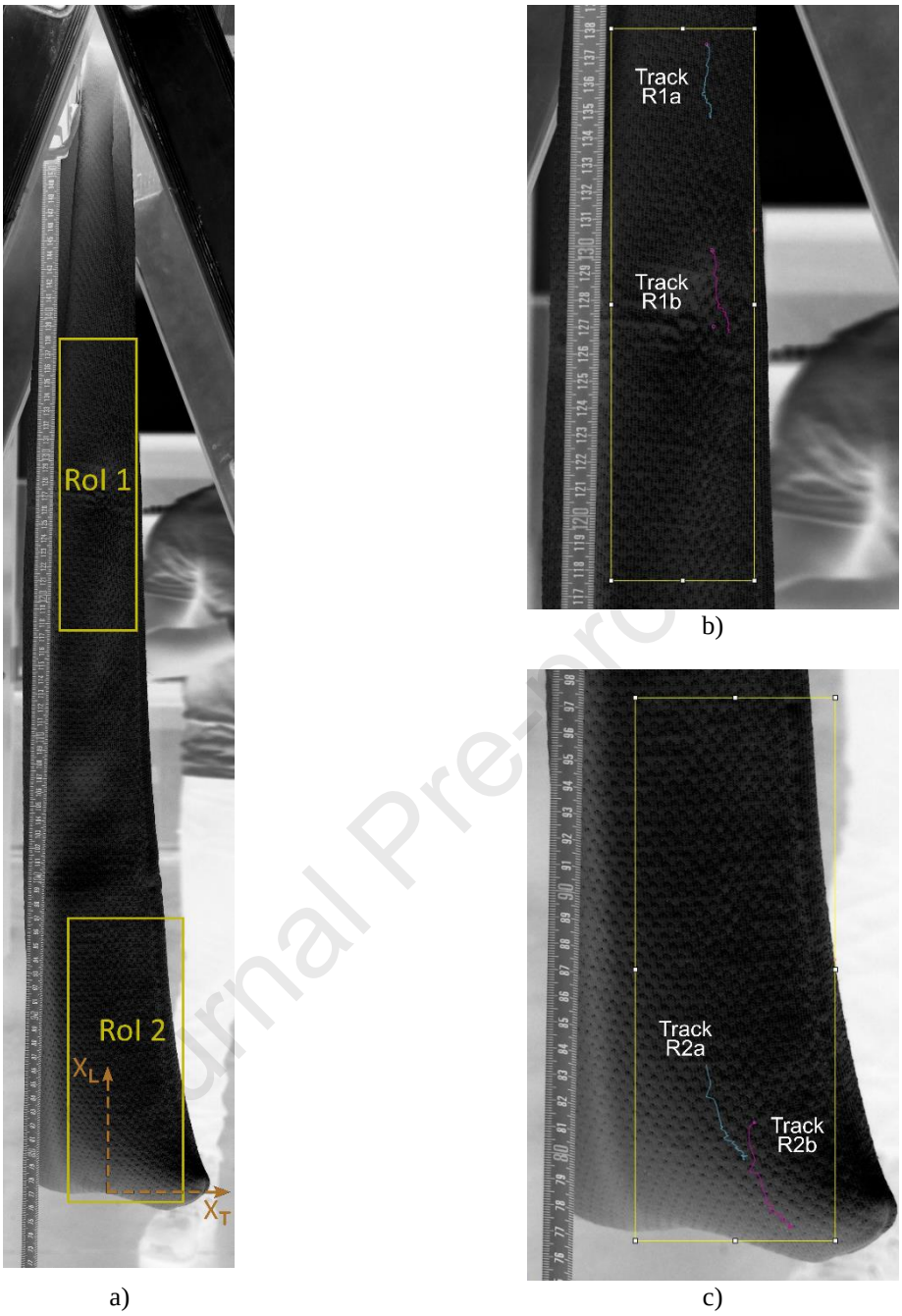


Figure 3. a) Fabric formwork RoIs and coordinates system relative to the end of the fabric formwork (longitudinal axis, $x_L$, and transverse axis, $x_T$), b) Tracks R1a and R1b obtained for RoI 1 and c) tracks R2a and R2b obtained for RoI 2.

569

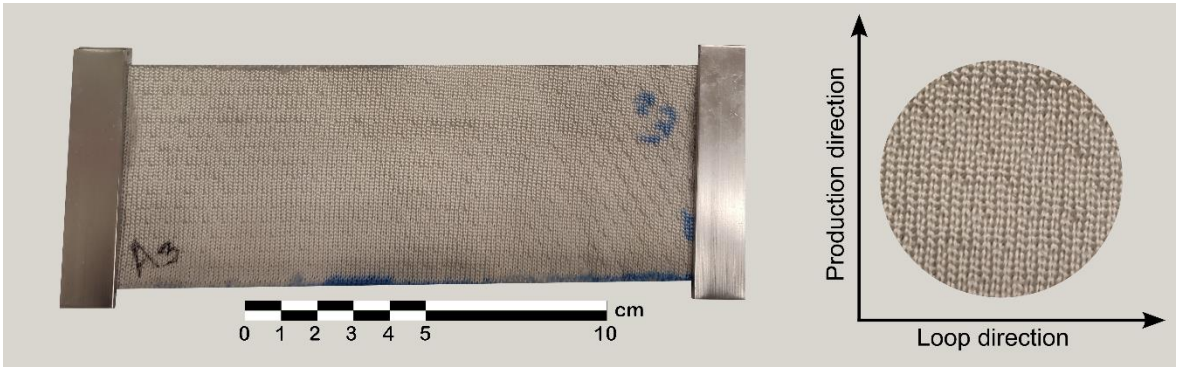


a)

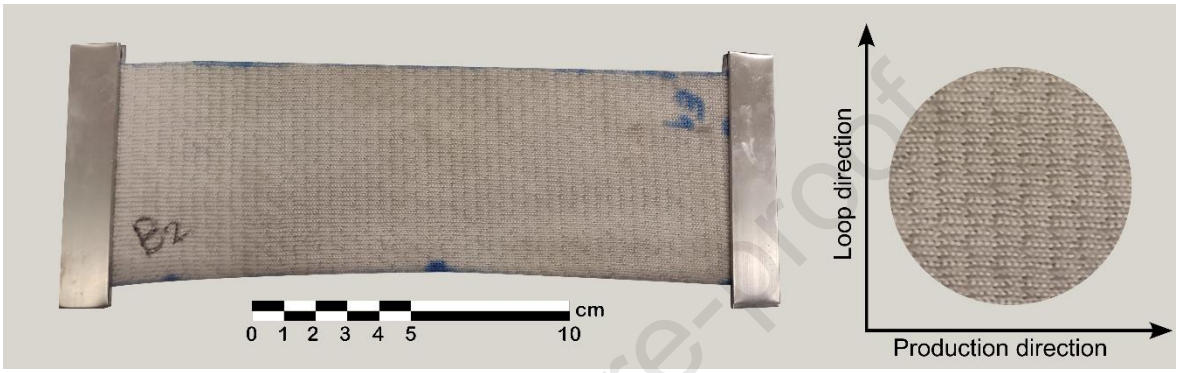


b)

Figure 4. a) Example of the specimens in the transverse direction and b) Example of the specimens in the longitudinal direction.

570

Figure 5. Tensile test set-up

571

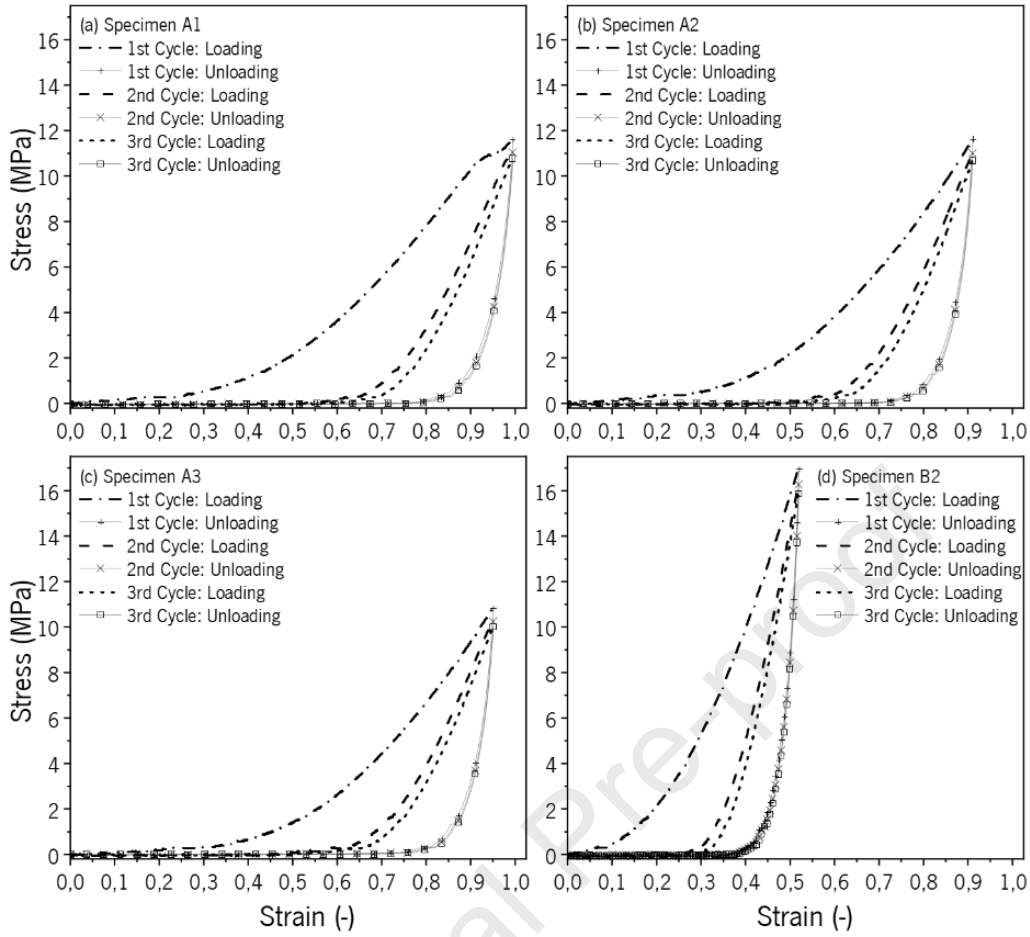


Figure 6. Stress vs. Strain responses obtained during the cyclic test of a) specimen A1, b) specimen A2, c) specimen A3, and d) specimen B2.

572

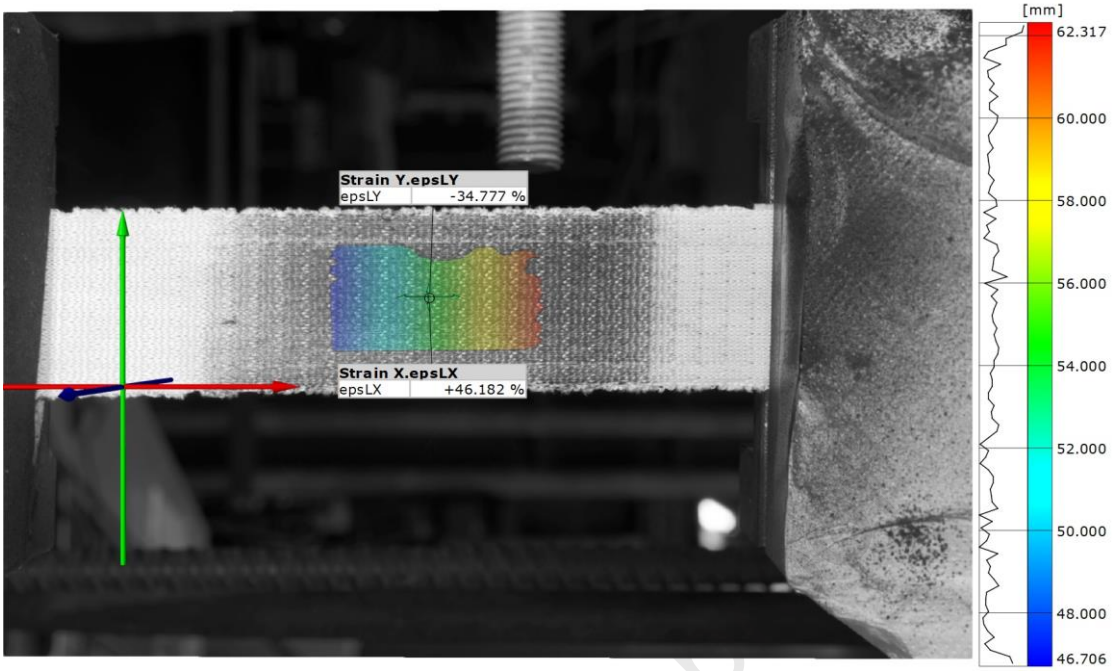


Figure 7. Image showing the longitudinal displacements field obtained right before the maximum elongation of the sample B2 was reached, during the first cycle of the uniaxial test.

573

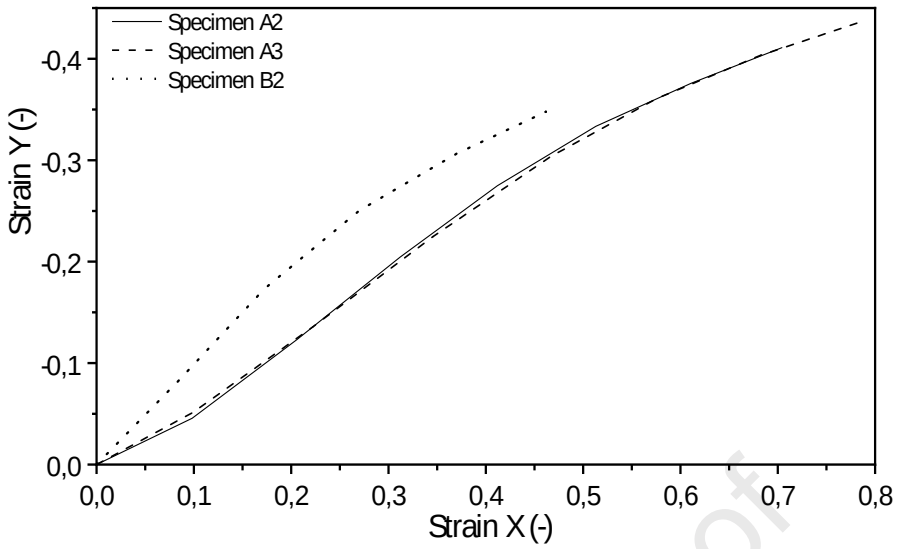


Figure 8. Strain Y vs Strain X during the first cycle of specimens A2, A3 and B2.

574

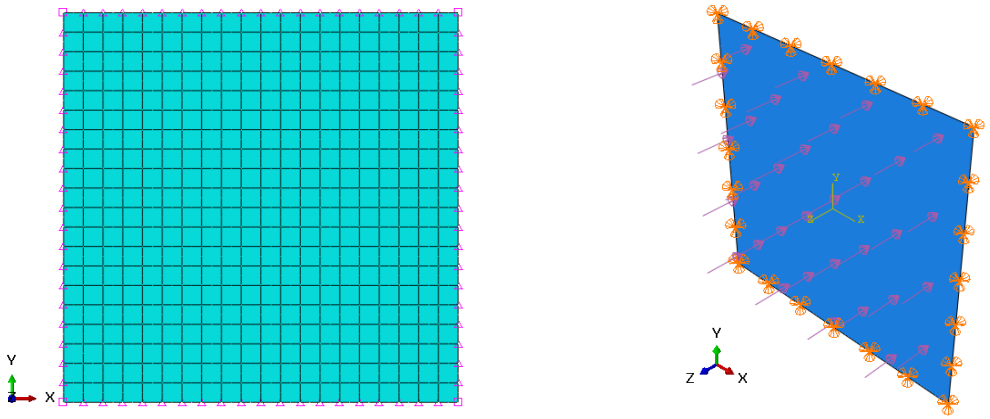


a) b)

Figure 9. a) uniform meshing and b) load and boundary conditions of the first model MI1.

575

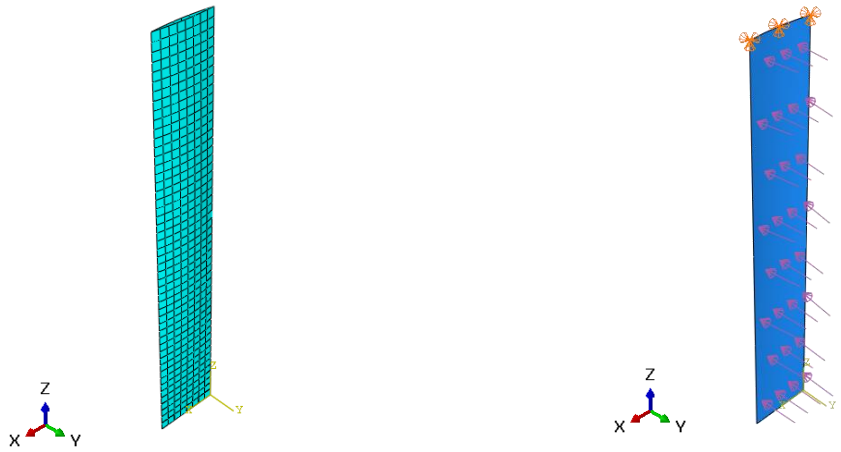


a) b)

Figure 10. a) Geometry and mesh of the Implicit model and b) Section in the XZ plane of the formwork where the boundary conditions and the load applied from the internal face are observed.

576

577

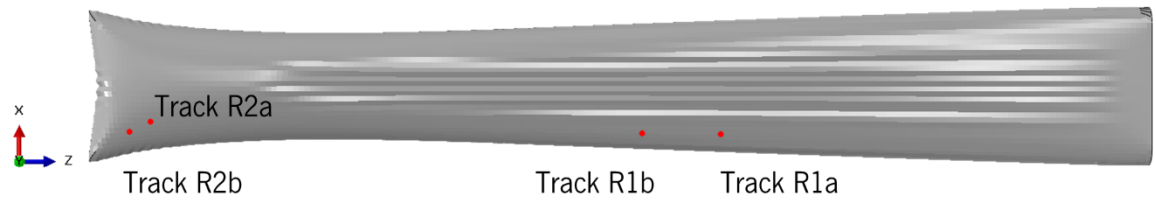


Figure 11. Approximate location on the numerical model of the points tracked in the experimental test.

578

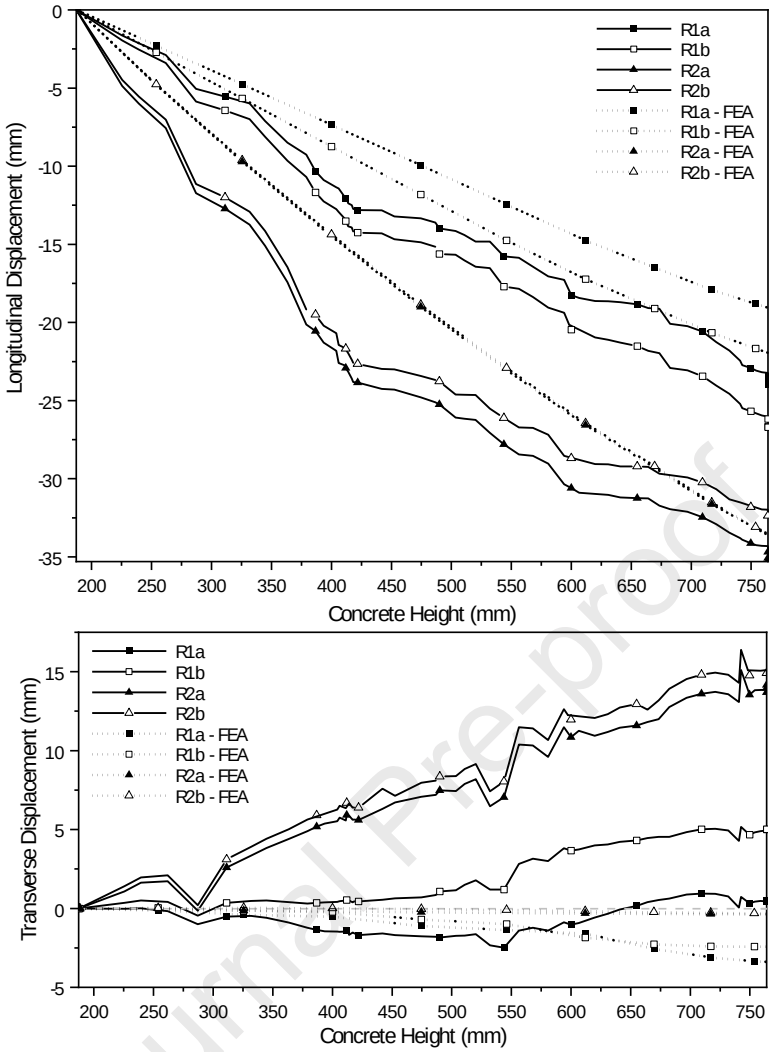


Figure 12. Comparison of the results obtained from the experimental analysis and the finite element model (FEA), in terms of: a) longitudinal displacements and b) transverse displacements with respect to the height of the mortar.

579

- This study assessed the feasibility of a systematic use of Knitted fabrics as flexible formworks for complex geometry concrete structures.
- This feasibility included the analysis of the mechanical properties of the constituent materials, the monitoring of the preform filling, and the numerical modelling of the structural interaction during filling, as a critical stage of the process.
- The mechanical properties of the knitted fabric were determined by experimental testing.
- The deformations at the surface of the fabric formwork were measured using Digital Image Techniques.
- The Finite Element Method was adopted to simulate the behavior of the casting process and a good agreement with the experimental results was obtained.

**Declaration of interests**

☒ The authors declare that they have no known competing financial interests or personal relationships that could have appeared to influence the work reported in this paper.

☐ The authors declare the following financial interests/personal relationships which may be considered as potential competing interests: